

Magnetic and Structural Studies of Vanadium Arene Complexes

Victoria Beck, Andrew R. Cowley, and Dermot O'Hare*

Chemistry Research Laboratory, Department of Chemistry, University of Oxford,
Mansfield Road, Oxford, U.K. OX1 3TA

Received April 8, 2004

The temperature dependence of the solid-state magnetic susceptibility for the paramagnetic V(I) complexes *trans*-(CpV)₂(μ-η⁶:η⁶-C₆H₆) (**1**) and CpV(η⁶-C₆H₆) (**2**) has been investigated. Complex **1** obeys the Curie–Weiss law over the temperature range 10–300 K with μ_{eff} = 4.81 μ_B and Θ = –18.8 K. The high-temperature moment is consistent with the presence of a total of four unpaired electrons derived from two low-spin V(I) d⁴ metal centers in an *S* = 2 configuration. However, at ca. 9 K the magnetic susceptibility displays a broad maximum. This magnetic behavior may be modeled over the full temperature range (4–300 K) using the Heisenberg intracluster magnetic exchange expression for an *S*₁ = *S*₂ = 1 system with *g* = 2.37, Θ = –12.3 K, and *J* = –2.64 cm^{–1}. Complex **2** obeys the Curie–Weiss law over the temperature range 5–300 K, with μ_{eff} = 2.86 μ_B and Θ = –5.0 K. The X-ray structure of **2** (*P*2₁/*a*, *a* = 10.7842(4) Å, *b* = 7.8233(4) Å, *c* = 11.2017(5) Å, β = 113.830(2)° at 150 K, *Z* = 4) has been determined. Crystals of **2** undergo a reversible phase transition to a new monoclinic cell with *a*' ≈ (*a* + *c*)/2, *b*' ≈ *b*, *c*' ≈ (*c* – *a*)/2 over the temperature range 290–270 K.

1. Introduction

The first triple-decker complex having an arene ring middle deck, *trans*-(CpV)₂(μ-η⁶:η⁶-C₆H₆) (**1**, Figure 1), was synthesized in 1983 by Jonas and co-workers.¹ Since then, many arene-bridged triple-decker complexes have been prepared.² However, few, if any, have been studied using magnetic susceptibility measurements to probe the presence of significant spin–spin exchange interactions between the metal centers in these complexes.

Many straight^{3a} triple-decker complexes conform to the 30/34-valence-electron (VE) rule of Hoffmann et al.⁴ and are thus predicted to be closed-shell, diamagnetic species (Figure 2a).⁵ Although Hoffmann's analysis does not predict a stable structure for the 26-VE complex **1**, a different MO scheme (Figure 2b) has since been determined for this complex by Chesky and Hall⁶ using nonempirical Fenske–Hall calculations and photoelec-

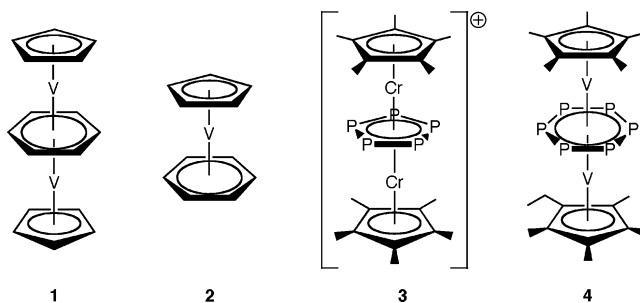


Figure 1. Triple-decker and related complexes with d⁴ metal centers.

tron (PE) spectra. The description of bonding is similar, but the order of the upper valence orbitals differs from that given by Hoffmann et al., whose order is incompatible with the photoelectron spectra. The PE spectra support the ground state 1δ_g²2σ_g¹3σ_u¹ with four unpaired electrons, the 1δ_g⁴ ground state being ruled out by the experimental PES data. Thus, **1** is predicted to be a stable, open-shell triple-decker complex.⁶

We are interested in investigating the magnetic properties of triple-decker complexes in which the metal centers are bridged by cyclic ligands that bring the metal centers into close proximity. Complex **1** is iso-electronic with the cationic triple-decker complex *trans*-(Cp*Cr)₂[μ-η⁵:η⁵-(cyclo-P₅)]⁺ (**3**; Figure 1), which undergoes a spin transition at an anion-dependent temp-

(5) However, several brief studies of the magnetic interactions in naphthalene-bridged lanthanide (slipped) triple-decker complexes have appeared: Bochkarev, M. N.; Fedushkin, I. L.; Fagin, A. A.; Schumann, H.; Demtschuk, J. *Chem. Commun.* **1997**, 1783–1784. Fedushkin, I. L.; Bochkarev, M. N.; Schumann, H.; Esser, L.; Kociok-Kohn, G. *J. Organomet. Chem.* **1995**, *489*, 145–151.

(6) Chesky, P. T.; Hall, M. B. *J. Am. Chem. Soc.* **1984**, *106*, 5186–5188.

* To whom correspondence should be addressed. Fax: 01865 285131. Tel: 01865 285130. E-mail: dermot.ohare@chem.ox.ac.uk.

(1) Duff, A. W.; Jonas, K.; Goddard, R.; Kraus, H. J.; Kruger, C. *J. Am. Chem. Soc.* **1983**, *105*, 5479–5480.

(2) For η⁶:η⁶-arene triple-decker complexes refer to the following references as well as ref 3b: Cibura, K.; Universitat Bochum, 1985. Lamanna, W. M. *J. Am. Chem. Soc.* **1986**, *108*, 2096–2097. Lamanna, W. M.; Gleason, W. B. *Organometallics* **1987**, *6*, 1583–1584. Cloke, F. G. N.; Courtney, K. A. E.; Sameh, A. A.; Swain, A. C. *Polyhedron* **1989**, *8*, 1641–1648. Wadepohl, H. *Angew. Chem., Int. Ed. Engl.* **1992**, *31*, 247–262. Priego, J. L.; Doerrler, L. H.; Rees, L. H.; Green, M. L. H. *Chem. Commun.* **2000**, 779–780.

(3) (a) A straight triple-decker complex exhibits pseudoaxial symmetry and equal bonding of both metal atoms to all ring atoms of the middle deck, e.g. *trans*-(CpV)₂(μ-η⁶:η⁶-C₆H₆);¹ on the other hand, the bonding of one or both metals to the bridging ring atoms in a slipped triple-decker complex is unequal, e.g. *trans*-(Cp*Co)₂(μ-η⁴:η⁴-C₆H₆).^{3b} (b) Schneider, J. J.; Denninger, U.; Heinemann, O.; Kruger, C. *Angew. Chem., Int. Ed. Engl.* **1995**, *34*, 592–595.

(4) Lauher, J. W.; Elian, M.; Summerville, R. H.; Hoffmann, R. *J. Am. Chem. Soc.* **1976**, *98*, 3219–3224.

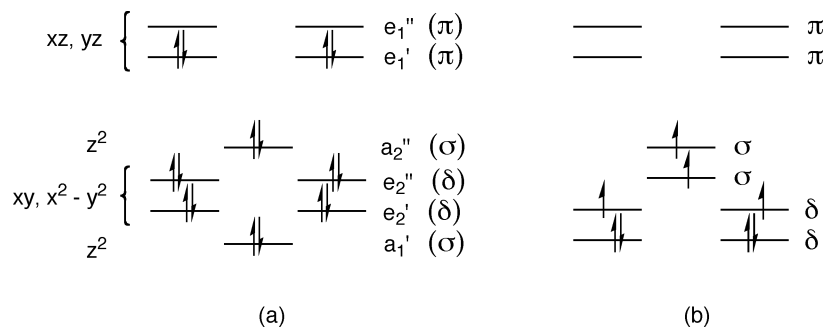


Figure 2. Molecular orbital schemes for (a) $trans\text{-}\{(\text{CpNi})_2(\mu\text{-}\eta^5:\eta^5\text{-Cp})\}^+$ (34 VE)⁴ and (b) $trans\text{-}(\text{CpV})_2(\mu\text{-}\eta^6:\eta^6\text{-C}_6\text{H}_6)$ (26 VE).⁷ The molecules are nearly cylindrical and therefore approach $D_{\infty h}$ symmetry; hence, the orbital labels σ , π , and δ can be used. The vertical energy scale is arbitrary.

erature.⁸ Given the similar geometries and electronic structures of **1** and **3**, it is postulated that **1** may also show interesting magnetic behavior. Only eight reports on **1** have appeared, including the original paper¹ and several theoretical studies,^{6,7,9} but no magnetic data are available for **1**. The synthesis and characterization of this complex, as well as those of its monomeric "building block" $\text{CpV}(\eta^6\text{-C}_6\text{H}_6)$ ¹⁰ (**2**) for comparison, were carried out.

2. Experimental Section

General Considerations. All reactions were performed under dinitrogen using Schlenk, glovebox, and vacuum line techniques. Solvents were distilled under dinitrogen from the appropriate drying agent: potassium (THF), sodium (*n*-heptanes, hexane), calcium hydride (EtOH). Solvents were thoroughly degassed before use by passage of a stream of dinitrogen through the solvent. High-resolution and electron impact mass spectra were recorded on a Micromass GCT calibrated with FC43, operating in electron impact mode with temperature-controlled addition to a solid probe. Fourier transform infrared spectra were recorded using a Perkin-Elmer FT1710 or a Perkin-Elmer FT1600 spectrometer (range 4000–400 cm^{-1}) as a Nujol mull between KBr plates. For these very air-sensitive compounds, the samples were prepared in a dinitrogen-filled glovebox; the spectra were run immediately. Solid-state magnetic susceptibility data were obtained using a Quantum Design MPMS-5 SQUID magnetometer. Accurately weighed powdered samples of ca. 0.05 g were loaded into gelatin capsules in a glovebox and placed between additional gelatin capsules in a nonmagnetic plastic straw, which was then lowered into the cryostat. The sample was therefore mounted in a weakly diamagnetic medium, and no correction was required for the diamagnetism of the sample holder. Magnetic susceptibility data were then measured at both 0.1 and 0.5 T. The measured data were corrected for the inherent diamagnetism of the sample by use of Pascal's constants.¹¹

Reagents. Vanadocene was prepared by the literature method.¹² *n*-Butyllithium (2.5 M in hexanes) was purchased from Aldrich and used as received.

Synthesis. $trans\text{-}(\text{CpV})_2(\mu\text{-}\eta^6:\eta^6\text{-C}_6\text{H}_6)$ (**1**). The complex $trans\text{-}(\text{CpV})_2(\mu\text{-}\eta^6:\eta^6\text{-C}_6\text{H}_6)$ (**1**) was prepared by the previously published method of Jonas et al.¹ MS (EI): m/z 310.0 (M^+ , 54%), 231.9 ($\text{M}^+ - \text{C}_6\text{H}_6$, 23%), 194.0 ($\text{M}^+ - \text{CpV}$, 40%), 181.0

($\text{M}^+ - \text{C}_6\text{H}_6\text{V}$, 41%), 116.0 ($\text{M}^+ - \text{C}_6\text{H}_6\text{VCp}$, 100%). IR: 1422 (w), 1365 (m), 1104 (s), 1054 (w), 1002 (s), 939 (s), 841 (w), 790 (m), 762 (vs), 669 cm^{-1} (w). Solid-state magnetic moment (SQUID, 300 K): 4.81 μ_B .

CpV($\eta^6\text{-C}_6\text{H}_6$) (2**).** A slightly modified literature procedure was employed for the synthesis of $\text{CpV}(\eta^6\text{-C}_6\text{H}_6)$ (**2**).¹⁰ To a solution of Cp_2V (3.54 g, 19.5 mmol) in THF (35 mL) was added 1,3-cyclohexadiene (2.77 mL, 29.25 mmol), followed by dropwise addition of $n\text{BuLi}$ (2.5 M in hexanes, 15.6 mL, 39 mmol) such that the solution became and remained hot but did not reflux. After the mixture had stood at room temperature for 1 h, it was cooled to 0 °C and dry, degassed EtOH (2.3 mL, 39 mmol) was added dropwise. The resulting orange-brown solution was then pumped to dryness at room temperature, and the solid residue was sublimed in vacuo at 75 °C to give a dark brown, crystalline solid (**2**). Yield: 2.599 g, 13.4 mmol (68.6%). Recrystallization from hexane at –35 °C yielded single crystals suitable for X-ray diffraction analysis. MS (EI): m/z 194.03 (M^+ , 15%), 116.0 ($\text{M}^+ - \text{C}_6\text{H}_6$, 50%), 78.0 ($\text{M}^+ - \text{CpV}$, 100%). High-resolution MS (EI) found (calculated): 194.0304 (194.0300), 1.9 ppm. IR: 1108 (s), 1007 (s), 978 (m), 950 (s), 845 (w), 781 (s), 750 (s), 699 cm^{-1} (w). Solid-state magnetic moment (SQUID, 300 K): 2.86 μ_B .

X-ray Data for CpV($\eta^6\text{-C}_6\text{H}_6$) (2**).** Crystals of **2** were grown by recrystallization from a hexane solution cooled to –35 °C. A crystal was mounted on a glass fiber using perfluoropolyether oil, transferred to a goniometer head on the diffractometer, and cooled rapidly to 150(2) K in a stream of cold N_2 using an Oxford Cryostream 600 series. Data collections were performed using an Enraf-Nonius FR590 Kappa CCD. The data were processed using the programs DENZO and SCALE-PACK.¹³ Structures were solved using the direct-methods program SHELXS¹⁴ and refined using full-matrix least-squares refinement on all F^2 data using SHELX-97. Examination of the systematic absences of the intensity data showed the space group to be $P2_1/a$. The structure was solved using the direct-methods program SIR92,¹⁵ which located all non-hydrogen atoms. Subsequent full-matrix least-squares refinement was carried out using the CRYSTALS program suite.¹⁶ Semi-empirical absorption corrections from equivalent reflections were carried out. Coordinates and anisotropic thermal parameters of all non-hydrogen atoms were refined. Examination of the resulting structure showed that the geometries of the ligands were distorted and that a large peak of excess electron

(7) Jemmis, E. D.; Reddy, A. C. *Organometallics* **1988**, *7*, 1561–1564.

(8) Hughes, A. K.; Murphy, V. J.; O'Hare, D. *J. Chem. Soc., Chem. Commun.* **1994**, 163–164.

(9) Reddy, A. C.; Jemmis, E. D. *Organometallics* **1992**, *11*, 3894–3900.

(10) Jonas, K.; Russeler, W.; Angermund, K.; Kruger, C. *Angew. Chem., Int. Ed. Engl.* **1986**, *25*, 927–928.

(11) O'Connor, C. J. *Prog. Inorg. Chem.* **1982**, *29*, 203–283.

(12) Floriani, C.; Mange, V. *Inorg. Synth.* **1990**, *28*, 263–267.

(13) Otwinowski, Z.; Minor, W. In *Methods in Enzymology*; Carter, C. W., Sweet, R. M., Eds.; Academic Press: New York, 1997; Vol. 276, pp 307–326.

(14) Sheldrick, G. M. SHELX97: Programs for Crystal Structure Analysis; Institut für Anorganische Chemie der Universität Göttingen, Göttingen, Germany, 1998.

(15) Altomare, A.; Cascarano, G.; Giacovazzo, G.; Guagliardi, A.; Burla, M. C.; Polidori, G.; Camalli, M. *J. Appl. Crystallogr.* **1994**, *27*, 435.

(16) Watkin, D. J.; Prout, C. K.; Carruthers, J. R.; Betteridge, P. W.; Cooper, R. I. CRYSTALS issue 11; Chemical Crystallography Laboratory, Oxford, U.K., 2001.

density was visible in a difference Fourier map. This was interpreted as being due to disorder of the entire molecule. In view of the high-temperature structure (see below) this was modeled as being disordered by inversion about a noncrystallographic center of inversion located at the site of the metal. Geometric restraints were applied to the coordinates of all carbon atoms in accordance with this model, and their coordinates and a common set of anisotropic thermal parameters for each symmetry-related pair were refined. The site occupancies were also refined subject to the constraints that the occupancies of all atoms of each orientation had a common value and that the total occupancy was unity. Hydrogen atoms were positioned geometrically after each cycle of refinement. A three-term Chebychev polynomial weighting scheme was applied. Refinement converged satisfactorily to give $R = 0.0471$ and $R_w = 0.0559$.

The same crystal was then warmed slowly (120 K h^{-1}) to 300 K. Determination of unit-cell parameters showed the crystal to adopt a monoclinic cell of approximately half the volume of the low-temperature form. The axes a' , b' , and c' of the small cell were related to those of the large cell, a , b , and c , by the transformations

$$a' \approx (a + c)/2$$

$$b' \approx b$$

$$c' \approx (c - a)/2$$

Intensity data were processed using the DENZO-SMN package.¹³ Examination of the systematic absences of the intensity data showed the space group to be $P2_1/n$. The structure was again solved using the direct-methods program SIR92.¹⁵ This showed the molecule to be disordered by a crystallographic center of inversion, with the vanadium atom located on the center. Examination of the other atoms located by direct methods showed that the structure could be interpreted as having three atoms of the Cp and C₆H₆ rings overlapping, while the remaining atoms were distinct. Coordinates of all 11 atoms were refined subject to geometric restraints (the geometries of the C₆ and C₅ rings were assumed to be a regular hexagon and pentagon, respectively, all V–benzene bonds were assumed to be of equal length, and all V–Cp bonds were assumed to be of equal length). The results of the structure determinations are displayed in Table 1.

3. Results and Discussion

The triple-decker complex $trans\text{-}(\text{CpV})_2(\mu\text{-}\eta^6\text{-}\eta^6\text{-C}_6\text{H}_6)$ (**1**) was prepared according to the method of Jonas and co-workers,¹ by the reaction of $\text{CpV}(\text{C}_3\text{H}_5)_2$ with an excess of 1,3-cyclohexadiene in refluxing *n*-heptanes. An adapted literature procedure was used to prepare the mixed-sandwich complex $\text{CpV}(\eta^6\text{-C}_6\text{H}_6)$ (**2**), from vanadocene and 1,3-cyclohexadiene.¹⁰

3.1. Structural Characterization. Crystals of **2** suitable for single-crystal X-ray analysis were grown by cooling a hexane solution to -35°C . The crystal structure for this known complex had not been previously reported. The crystals undergo a reversible phase change over the temperature range 290–270 K. However, there is still substantial disorder below this temperature. While the extent of this presumably decreases on further cooling, it is unclear whether the crystal would ever become completely ordered. Between 270 and 290 K, the diffraction pattern shows a considerable amount of structured diffuse scatter, suggesting that there is local ordering of the molecules, although this does not extend sufficiently far through the crystal to give well-defined Bragg peaks. The diffuse scatter is

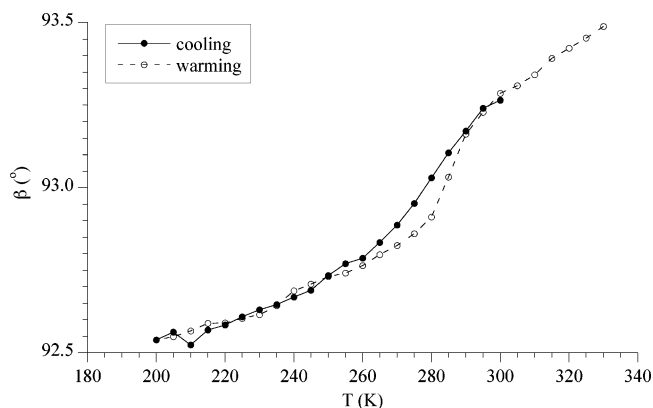


Figure 3. Temperature dependence of β for a single crystal of **2**.

Table 1. Crystal Data and Refinement Details for **2**

	150 K	300 K
Crystal Data		
empirical formula	C ₁₁ H ₁₁ V	C ₁₁ H ₁₁ V
formula wt	194.15	194.15
cryst syst	monoclinic	monoclinic
space group	$P2_1/a$	$P2_1/n$
<i>a</i> (Å)	10.7842(4)	6.1021(2)
<i>b</i> (Å)	7.8233(4)	7.8936(4)
<i>c</i> (Å)	11.2017(5)	9.4253(5)
β (deg)	113.630(2)	93.2639(17)
cell volume (Å ³)	865.8	453.3
<i>Z</i>	4	2
calcd density (Mg/m ³)	1.489	1.422
<i>F</i> ₀₀₀	401.107	200.553
cryst size (mm)	0.16 × 0.24 × 0.32	0.16 × 0.24 × 0.34
descripn of cryst	black block	black block
Data Collection		
<i>T</i> (K)	150	300
radiation (λ , Å)	0.717 03	0.710 73
monochromator	graphite	graphite
θ range for data collection (deg)	$5.0 \leq \theta \leq 27.5$	$5.0 \leq \theta \leq 27.5$
Refinement		
no. of rflns measd	6344	3603
no. of unique rflns	2091	1084
no. of obsd rflns ($I > 3\sigma(I)$)	1588	813
no. of params refined	143	106
<i>R</i> _{int}	0.024	0.017
<i>R</i>	0.0471	0.0246
<i>R</i> _w	0.0559	0.0357
goodness of fit	1.0341	0.8257
min, max resid electron density (e Å ⁻³)	-0.65, 0.83	-0.22, 0.13

largely removed by heating to 300 K. At higher temperatures the diffraction pattern rapidly weakens, suggesting that atomic positions become poorly defined as a result of thermal motion and/or more extensive disorder.

The temperature dependence of the monoclinic cell angle β is shown in Figure 3.

The discontinuity (from ca. 260–290 K) in β is associated with partial ordering of the molecule in the crystal. The sigmoidal curve shape is characteristic of a second-order phase change, but the thermal hysteresis over the discontinuity temperature range is not. This hysteresis effect may result from kinetic considerations; it is possible that the crystal was cooled too quickly to reach equilibrium, resulting in the high-temperature structure being “frozen in.” The other cell parameters

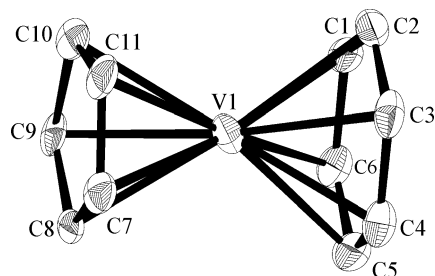


Figure 4. Plot of the thermal probability ellipsoids (50% probability) for **2**. The view is of the more highly occupied orientation of the molecule at 150 K. Hydrogen atoms are omitted for clarity.

Table 2. Selected Bond Lengths and Other Structural Parameters for **2 (Major Occupancy, 150 K)**

Bond Lengths (Å)			
V(1)–C(1)	2.207(3)	V(1)–C(7)	2.252(3)
V(1)–C(2)	2.202(3)	V(1)–C(8)	2.250(3)
V(1)–C(3)	2.200(3)	V(1)–C(9)	2.259(3)
V(1)–C(4)	2.221(3)	V(1)–C(10)	2.238(3)
V(1)–C(5)	2.264(3)	V(1)–C(11)	2.217(3)
V(1)–C(6)	2.234(3)		
Other Structural Parameters (Å)			
V(1)⋯Cp ^a	1.89	V(1)⋯C ₆ H ₆ ^a	1.72

^a Denotes the distance from the V center to the ring centroid.

(*a*, *b*, *c*, cell volume) show the same trend in temperature dependence as *β*, although not so clearly. There is much precedent for this phenomenon in crystallographic studies of transition-metal sandwich compounds. Ferrocene itself exhibits similar behavior.¹⁷

The low-temperature structure (*vide supra*) is shown in Figure 4, and selected bond distances and other structural parameters are given in Table 2.

The molecule has a highly regular structure, in which the Cp and C₆H₆ rings are approximately parallel (the interplanar angle at 150 K is 1.4°) and are symmetrically bonded to the metal. The vanadium atom lies slightly closer to the C₆H₆ ring than to the Cp ring (the shortest distances from the metal to the best planes of the C₆H₆ and Cp ligands are 1.72 and 1.89 Å, respectively, at 150 K). Although the difference is somewhat less pronounced in **2**, the same pattern of V–ring centroid distances was also seen in **1** (V–C₆H₆, 1.702 Å; V–Cp, 1.922 Å).¹ This is similar to what is seen for the triple-decker compound *trans*-(CpV)(*μ*-η⁶:η⁶-C₆H₆)-[Li(TMEDA)],¹⁰ in which the V–C₆H₆(centroid) distance is 1.590 Å and the V–Cp(centroid) distance is 1.920 Å.

The mean V–C distance from the metal to the Cp ring in **2** is 2.243 Å; the mean V–C distance for the benzene ring is 2.221 Å. The latter value is only marginally shorter than the mean V–C_{benzene} distance found in **1** (2.233 Å).¹ Likewise, the distance from the V atom to the plane of the benzene ring in **2** (1.72 Å) is only slightly longer than the corresponding distance in **1** (1.702 Å).¹ This indicates that coordination of the benzene ring by two vanadium atoms does not weaken to any great extent the bonding of the individual V(I) centers to this ring. This is unusual; in most triple-

(17) Seiler, P.; Dunitz, J. *Acta Crystallogr., Sect. B* **1979**, *35*, 2020. Seiler, P.; Dunitz, J. *Acta Crystallogr., Sect. B* **1982**, *38*, 1741. Ebsworth, E. A. V.; Rankin, D. W. H.; Cradock, S. *Structural Methods in Inorganic Chemistry*, 2nd ed.; Blackwell Scientific: Oxford, U.K., 1991.

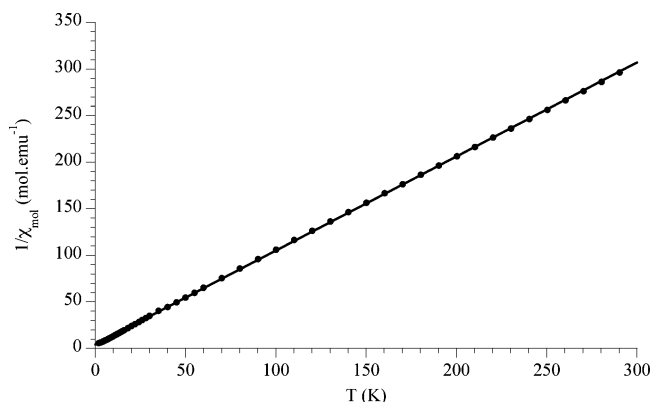


Figure 5. Plot of χ_{mol}^{-1} vs *T* for **2**. The line is a fit to the Curie–Weiss law between 5 and 300 K.

deckers, the M–C distance to the middle deck is longer than the M–C distance to the same ring ligand in the corresponding monometallic species. In slipped triple-decker complexes with bicyclic middle decks, the bonds from the metal centers to the bridgehead carbon atoms of the bridging ligand (i.e. those carbons shared by *both* metal centers) are similarly elongated.

3.2. Magnetic Properties. The temperature dependence of the solid-state magnetic susceptibility for CpV(η⁶-C₆H₆) (**2**) was measured using SQUID magnetometry. The Curie–Weiss plot for **2** is linear over the entire temperature range (Figure 5). For this complex, the Curie constant is *C* = 1.02 emu K/mol and the Weiss temperature is Θ = –5.0 K. The derived value of μ_{eff} is 2.86 μ_{B} , consistent with an intermediate-spin d⁴ metal center in a uniaxial (cylindrical) ligand field (cf. chromocene (e₂)³(a₁)¹(e₁)⁰; μ_{so} = 2.83 μ_{B}). The room-temperature magnetic moment falls within the range observed for other magnetically characterized mononuclear V(I) complexes (2.59–2.91 μ_{B}).¹⁸

The triple-decker complex **1** was found to be EPR silent at room temperature (toluene solution). Measurements of μ_{eff} in solution by the Evans NMR method were precluded by the exceedingly low solubility of the compound (8 g/L boiling toluene).¹ The predicted ground state for this triple-decker sandwich complex is, on the basis of PE spectra, 1 $\delta_{\text{g}}^2 2\sigma_{\text{g}}^2 13\sigma_{\text{u}}^1$; the alternative closed-shell ground state, 1 δ_{g}^4 , is ruled out.^{6,19,20} Therefore, it is expected that four unpaired electrons will be observed for **1** with an *S* = 2 configuration.

Solid-state magnetic susceptibility data were collected for a sample of **1** between 4 and 300 K using a SQUID magnetometer. The temperature dependence of the molar magnetization for **1** was measured at both 0.1 and 0.5 T, after cooling in zero field and in a field. We noted no difference in the observed magnetic susceptibility of the sample under any of these conditions.

(18) For examples of magnetically characterized monometallic V(I) complexes see: Gordon, D. C.; Deakin, L.; Arif, A. M.; Miller, J. S. *J. Am. Chem. Soc.* **2000**, *122*, 290–299. Barybin, M. V.; Young, V. G.; Ellis, J. E. *J. Am. Chem. Soc.* **1998**, *120*, 429–430. Calderazzo, F. *Inorg. Chem.* **1964**, *3*, 810–814. Calderazzo, F.; Debenedetto, G. E.; Pampaloni, G.; Mossmer, C. M.; Strahle, J.; Wurst, K. *J. Organomet. Chem.* **1993**, *451*, 73–81. Calderazzo, F.; Invernizzi, R.; Marchetti, F.; Masi, F.; Moalli, A.; Pampaloni, G.; Rocchi, L. *Gazz. Chim. Ital.* **1993**, *123*, 53–60. Calderazzo, F.; Debenedetto, G. E.; Detti, S.; Pampaloni, G. *J. Chem. Soc., Dalton Trans.* **1997**, 3319–3324.

(19) Jemmis, E. D.; Reddy, A. C. *Proc. Indian Acad. Sci. (Chem. Sci.)* **1990**, *102*, 379–393.

(20) Warren, K. D. *Inorg. Chem.* **1974**, *13*, 1317–1324.

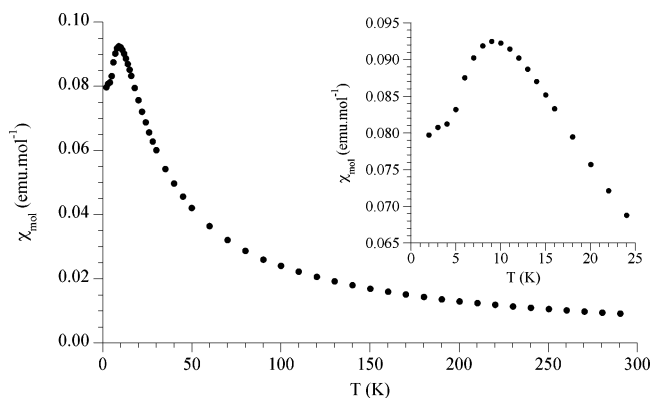


Figure 6. Plot of χ_{mol} vs T for **1** (zero-field-cooled data, $H = 0.1$ T).

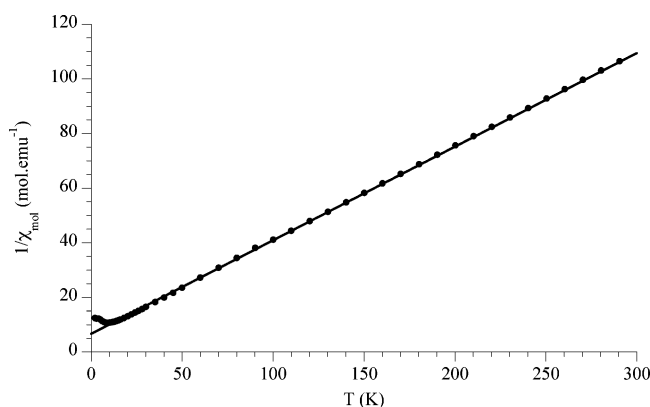


Figure 7. Plot of χ_{mol}^{-1} vs T for **1**. The line is a least-squares fit to the Curie–Weiss law between 10 and 300 K.

The plot of χ_{mol} versus T for **1** is given in Figure 6. Above 10 K the molar magnetic susceptibility data can be fitted to the Curie–Weiss law with $C = 2.89$ emu K/mol and a Weiss constant $\Theta = -18.6$ K (Figure 7). This gives a value of μ_{eff} for **1** of $4.81 \mu_{\text{B}}$. The effective spin-only magnetic moment for two noninteracting low-spin ($S_1 = S_2 = 1$) metal centers is given by $\mu_{\text{eff}}^2 = \{g_1^2 S_1(S_1 + 1) + g_2^2 S_2(S_2 + 1)\}$; for $g_1 = g_2 = 2$ and $S_1 = S_2 = 1$ this gives $\mu_{\text{eff}} = 4.0 \mu_{\text{B}}$. On the other hand if we have an $S = 2$ ground state, the effective spin-only moment would be $4.89 \mu_{\text{B}}$, which is close to the value observed. The $S = 2$ ground state is therefore assigned to **1**.

At ca. 9 K the molar magnetic susceptibility reaches a maximum. A maximum in χ_{mol} at low temperatures is often observed for solids that exhibit spin-glass or long-range antiferromagnetic behavior. Spin-glass behavior is unlikely, as we see no difference in the zero-field-cooled and field-cooled susceptibility data sets. Given the molecular nature of the solid, we believe an intramolecular antiferromagnetic spin–spin interaction is more likely.

For a system with two paramagnetic centers, the isotropic Hamiltonian is $\mathbf{H} = -2J\mathbf{S}_1 \cdot \mathbf{S}_2$, where J is the exchange constant and measures the strength of the spin interaction and \mathbf{S}_1 and \mathbf{S}_2 represent the spin operators of the two paramagnetic atoms in the dimer. The expression describing the magnetic susceptibility per mole of $S_1 = S_2 = 1$ dimers (eq 1) is arrived at by

$$\chi = [2Ng^2\mu_{\text{B}}^2/k(T - \Theta)](e^{2J/kT} + 5e^{6J/kT})(1 + 3e^{2J/kT} + 5e^{6J/kT})^{-1} \quad (1)$$

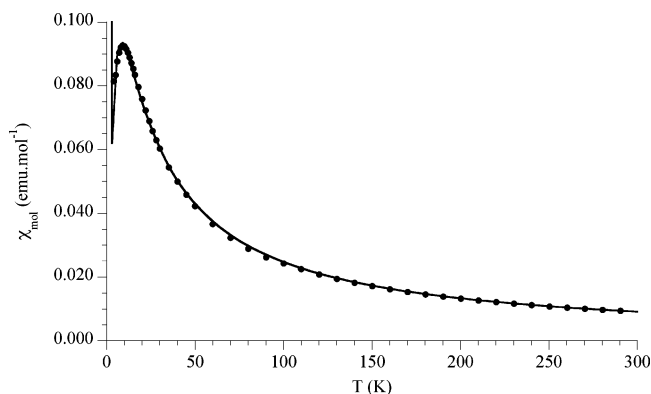


Figure 8. Least-squares fit (solid line) of χ_{mol} data for **1** to eq 1. The fit was performed for $T \geq 4$ K. Found: $g = 2.37$; $\Theta = -12.3$ K; $J = -2.64$ cm $^{-1}$. Goodness of fit: $R = 0.9999$ ($\chi^2 = 9.49 \times 10^{-6}$).

solving the Van Vleck equation using the isotropic Hamiltonian.²¹ The expression is relatively simple, since there is only one J value. Because inversion symmetry is present in **1**,¹ the analysis is further simplified; $S_1 = S_2 = 1$ and $g_1 = g_2$. N is Avogadro's number, μ_{B} is the Bohr magneton, k is the Boltzmann constant, $2|J|$ is the energy separation between the ground state and the excited state, and Θ is the Weiss constant.

A least-squares fit of the χ_{mol} data for **1** between 4 and 300 K to eq 1 is shown in Figure 8. The fitted parameters are $g = 2.37$, $\Theta = -12.3$ K, and $J = -2.64$ cm $^{-1}$.

We were not able to extend the fit below 4 K, due to the presence of a small amount of a paramagnetic Curie impurity.

The negative Weiss constant ($\Theta = -12.3$ K) indicates that there are short-range antiferromagnetic interactions between molecules,²¹ while the negative value of J indicates that intramolecular coupling is antiferromagnetic, giving an $S = 0$ ground state at low temperature. The broad maximum in χ_{mol} ($T_{\text{N}} = 9$ – 10 K) is comparable²¹ to the energy separation between the $S = 0$ ground state and the $S = 2$ excited state ($2|J| = 8$ K). Given that the V(I) centers are brought into relatively close proximity by a bifacially bonded π -perimeter ligand, the value of J (-2.64 cm $^{-1}$) is surprisingly small. The effect of metal–metal separation on magnetic exchange is discussed below.

Complex **1** is isoelectronic with the cationic triple-decker complex $\text{trans}\{(\text{Cp}^*\text{Cr})_2[\mu\text{-}\eta^5\text{-}\eta^5\text{-}(\text{cyclo-P}_5)]\}^+$ (**3**), which exhibits two spin-crossover transitions ($\text{LS:LS} \leftrightarrow \text{LS:HS} \leftrightarrow \text{HS:HS}$).²² The magnetic transitions show thermal hysteresis and are anion-dependent.⁸ At high temperatures (150–300 K), the molar susceptibility data for **3** were fitted to the Curie law with $\mu_{\text{eff}} = 4.1 \mu_{\text{B}}$, which is consistent with two noninteracting low-spin d^4 ($S = 1$) Cr centers.⁸ In contrast, the vanadium complex **1** does not exhibit evidence of a two-stage crossover, nor does it exhibit thermal hysteresis.

Clearly, the difference in the structures and electronic nature of the two complexes undoubtedly affects the degree and type of magnetic interaction found. The

(21) Carlin, R. L. *Magnetochemistry*; Springer-Verlag: Berlin, 1986.
(22) O'Hare, D.; Barlow, S.; Hughes, A. K.; Manners, I.; Honeyman, C. H.; Pudelski, J. K.; Lough, A. J. *Applications of Organometallic Chemistry in the Preparation and Processing of Advanced Materials*; NATO ASI Series; Plenum: New York, 1995; p 311.

distance between the Cr²⁺ centers in **3** (3.185 Å)⁸ is shorter than the distance between the V⁺ centers in **1** (3.403 Å)¹ (which is not entirely unexpected due to the smaller ionic radius of Cr²⁺ compared to V⁺, as well as the larger size of the phosphorus atoms in P₅ compared to the carbon atoms in C₆H₆, despite the difference in ring size). Complex **1** is also isoelectronic with the (diamagnetic) triple-decker complexes *trans*-(Cp'V)₂[μ-η⁶:η⁶-(*cyclo*-P₆)] shown in Figure 1 (**4**, Cp' = η⁵-C₅Me₄-Et; also known for Cp' = Cp, Cp*, η⁵-C₅H₄Me, η⁵-C₅H₄^tBu, η⁵-C₉H₇).^{23,24} In **4**, the V–V distance (2.627(2) Å) is shorter still than in **1**, as expected due to the larger size of the P₆ ring relative to benzene. This decrease in intermetallic distance appears to have the effect of strengthening the antiferromagnetic coupling between the metal centers to the point where the molecule is diamagnetic at room temperature.²³ The same observation is made when Cp' = Cp*.²⁴

In terms of the dependence of spin state on M–M distance (M = V, Cr) in these 26-VE triple-deckers, it appears that a distance of ca. 3.1–3.2 Å is optimal for spin crossover. Longer separations lead to weak anti-ferromagnetic coupling at low temperature, and shorter separations result in a diamagnetic ground state. Indeed, it has been proposed that the magnitude of the internuclear distance in a binuclear complex will impose a limit on the maximum magnitude of *J*.^{11,25} However, much work has been carried out on magnetic exchange, and the results indicate that intermetallic separation may not directly affect the magnitude of magnetic coupling, the chemical nature of the ligand bridge

(23) Scherer, O. J.; Schwalb, J.; Swarowsky, H.; Wolmerschauser, G.; Kaim, W.; Gross, R. *Chem. Ber.* **1988**, *121*, 443–449.

(24) Herberhold, M.; Frohmader, G.; Milius, W. *J. Organomet. Chem.* **1996**, *522*, 185–196.

(25) Coffman, R. E.; Buettner, G. R. *J. Phys. Chem.* **1979**, *83*, 2387–2392.

usually having the larger effect.¹¹ The geometry, composition, and electronic character of the bridging ligands differ greatly among **1**, **3**, and **4**. In addition, the ordering and relative energies of the molecular orbitals for various closely related triple-decker sandwich complexes have been correlated; the study by Jemmis and Reddy,¹⁹ which included **1** and **3**, showed that the identities of the metals and of the bridging ligand profoundly affect the MOs for these species. The relative energies of the frontier orbitals are therefore different for the two complexes, leading to different magnetic properties.

4. Conclusion

The magnetic properties of the vanadium(I) arene complexes *trans*-(CpV)₂(μ-η⁶:η⁶-C₆H₆) (**1**) and CpV(η⁶-C₆H₆) (**2**) have been studied by variable-temperature solid-state magnetometry. Both complexes contain V(I) d⁴ metal centers. In **2** the spins are relatively isolated and obey the Curie–Weiss law over the entire temperature range (4–300 K). For **1**, the close proximity of the two V(I) centers bridged by the arene ligand gives rise to more complex magnetic behavior. The magnetic data can be fitted to a Heisenberg S₁ = S₂ = 1 dimer model. Intermetallic separation in the 26-VE triple-decker complexes **1**, **3**, and **4** appears to affect the degree of magnetic exchange observed, with shorter separations leading to spin-crossover and ultimately diamagnetism.

Supporting Information Available: Tables giving anisotropic thermal parameters, positional and thermal parameters, and bond lengths and angles for the high- and low-temperature structures of CpV(η⁶-C₆H₆). This material is available free of charge via the Internet at <http://pubs.acs.org>.

OM0497442